PHYSICAL REVIEW B VOLUME 50, NUMBER 16 15 OCTOBER 1994-II

Improved modeling of excitons in type-II semiconductor heterostructures by use of a three-dimensional variational function

Abdsadek Bellabchara, Pierre Lefebvre, Philippe Christol, and Henry Mathieu
Groupe d'Etude des Semiconducteurs, Université Montpellier II–CNRS, Case 074, 34095 Montpellier Cedex 5, France

(Received 22 February 1994; revised manuscript received 3 June 1994)

Binding energies and oscillator strengths of excitons in staggered-lineup heterostructures such as type-II quantum wells are calculated by a variational method, using a single parameter. This method involves the effective attractive potential imposed by the confined carrier to its unconfined companion. Contrary to previous comparable works, a three-dimensional trial function of the variable r ($r=|\mathbf{r}_e-\mathbf{r}_h|$) is used, instead of a two-dimensional function of the in-plane projection ρ. Due to the large spatial extension along z of the wave function of the unconfined carrier, the latter approximation commonly used up to date, is too drastic, even though it works reasonably well for type-I systems. This is demonstrated by comparison of both hypotheses for GaAs-AlAs systems: when using the 3D function, binding energies are increased by up to 52%, while electron-hole overlap integrals can be enhanced by one order of magnitude.

I. INTRODUCTION

The increasing variety of strained or unstrained semiconductor quantum wells and superlattices that can be grown, allows us to produce several physical configurations, which may all be of interest for device applications. For instance, depending on the lineup of band extrema, different localizations of electrons and holes can occur. The most widely studied case is the so-called type-I lineup, where electrons and holes are confined within the same layers and buildup excitons with larger binding energies and oscillator strengths than in the corresponding bulk material. Now there is a growing interest in the so-called type-II case, where both carriers are maintained apart in two adjacent materials.[1–17] This separation induces a loosening of the Coulombic binding and a dramatic breakdown of oscillator strength, which could be recovered by applying a longitudinal electric field, with a large modulation contrast. Type-II situations originate from various mechanisms, like the presence of internal strains or simply the natural alignment of different conduction- or valence-band extrema. For instance, in GaAs-AlAs structures[1,3–10,14,16] the hole states are always localized within the GaAs layers; this is also true for electron states builtup from states near the Γ point of host materials, so that type-I excitons are produced. On the other hand, electrons originating from X states of the Brillouin zone are rather localized within AlAs layers, which leads to a type-II electron-hole pair. Depending on the various layer thicknesses,[16] the fundamental valence- to conduction-band energy gap of the structure may be either type I or type II. Another example is given by strained CdTe-(Cd,Zn)Te heterostructures, for which previous works have evidenced a mixed situation, due to interfacial biaxial strains: heavy-hole excitons are type I, while light-hole excitons are type II.[17] More recently, several studies[12,13,15] of CdTe-(Cd,Mn)Te quantum wells have shown the continuous change from type I to type II provoked by the giant effect of an external magnetic field on the valence states of (Cd,Mn)Te.

From the theoretical viewpoint, several methods, all based on the variational theorem, have been proposed for calculating the characteristics of the 1s exciton state in such staggered-lineup systems.[1–15] Early attempts[1] assumed infinitely high potential barriers, which allows easy calculation of binding energies but prohibits any estimation of oscillator strengths or of the exchange interaction. Most other models include finite band offsets but basically depend on a prior determination of electron and hole envelope functions,[1,3,4,7–12] which requires that both carriers are confined in respective quantum wells. This is the case for short period superlattices but not for single type-II quantum wells, where one of the carriers is only bound to its confined companion by Coulomb attraction. The artificial "envelope function" of this quasibound carrier then has to be part of the trial function, introducing one or several additional variational parameters.[2,5,6] As a whole, most methods use more than one parameter, and/or expansions on bases of well-behaved functions, and are thus time consuming.

Recently, alternative methods[13–15] were proposed, based on the adiabatic approximation[18] of the effective Coulomb potential created by the confined carrier. Numerical calculations of the confinement of the other carrier in this potential then provide the binding energy and a reasonable shape of the total wave function, using a single parameter. In this work, we introduce a comparable approach, using less restrictive hypotheses than previously done. We perform an exact calculation within the effective-potential context, but use a three-dimensional (3D)-like trial function instead of a 2D-like one.[18] We show that this constitutes a serious improvement, regarding the variational principle, since binding energies can be increased by ~50%, while oscillator strengths can be multiplied by a factor of ~10, in the case of GaAs-AlAs structures.

0163-1829/94/50(16)/11840(5)/$06.00

II. CALCULATION OF EXCITON BINDING ENERGY

We shall consider the case of a single quantum well. For convenience, in the following, the hole is taken confined in a well, while the electron faces a potential barrier, as in the example of X-like states in GaAs-AlAs structures. Of course, all calculations are reversible in terms of electrons and holes, and still stand for multiple quantum wells, superlattices, or even type-I systems.[18] Within the standard envelope-function formalism, the exciton function $\Phi_{\mathrm{ex}}(\mathbf{r}_e,\mathbf{r}_h)$ describing the in-plane relative motion is solution of the following effective-mass equation:

$$\left\{-\frac{\hbar^2}{2}\left[\frac{\partial}{\partial z_e}\left[\frac{1}{m_{ez}}\frac{\partial}{\partial z_e}\right]+\frac{\partial}{\partial z_h}\left[\frac{1}{m_{hz}}\frac{\partial}{\partial z_h}\right]\right]-\frac{\hbar^2}{2\mu_\perp}\nabla_\rho^2 + V_e(z_e)+V_h(z_h)-\frac{e^2}{\varepsilon_r|\mathbf{r}_e-\mathbf{r}_h|}\right\}\Phi_{\mathrm{ex}}=E_{\mathrm{ex}}\Phi_{\mathrm{ex}} \ , \tag{1}$$

where z_e, z_h are, respectively, the coordinates along the growth axis (z,z') of the structure of the electron and the hole, and ρ the in-plane relative coordinate. m_{ez} and m_{hz} are the effective masses for the motion along z. The hermiticity of the effective-mass Hamiltonian imposes the general form of the two first kinetic energy terms in Eq. (1).[19,20] Nevertheless, in practice, the on-axis effective masses m_{ez} and m_{hz} have z-independent values within each material, which leaves us with simple second-derivative operators. The eventual mass mismatch at the interface between two layers can be included by particular boundary conditions, namely the continuity of the envelope function itself and of the probability current.[19,20] Concerning the electron-hole reduced mass for the in-plane motion $\mu_\perp$ we can take an intermediate value of the corresponding kinetic energy by averaging $(\mu_\perp)^{-1}$ over the whole structure. $V_e(z_e)$ and $V_h(z_h)$ are the respective conduction and valence potential profiles and ε_r the background dielectric constant, which can be taken as the mean of the values for both materials, as long as image-charge effects are neglected.[14] In all comparable works on type-II quantum wells,[12-14] the ansatz, hereafter called the 2D approximation, chosen for the shape of $\Phi_{\mathrm{ex}}(\mathbf{r}_e,\mathbf{r}_h)$, allowed the following separation of in-plane and on-axis motions:

$$\Phi_{\mathrm{ex}}(\mathbf{r}_e,\mathbf{r}_h)=f_e(z_e)f_h(z_h)\varphi_{\mathrm{2D}}(\rho) \ , \tag{2}$$

where $f_h(z_h)$ is the normalized hole envelope function, corresponding to the eigenenergy E_h, and $\phi_{\mathrm{2D}}(\rho)$ is the normalized 2D hydrogenic 1s-like wave function, containing the variational extension parameter $\alpha_\perp$

$$\varphi_{\mathrm{2D}}(\rho)=\frac{2}{\alpha_\perp}e^{-\rho/\alpha_\perp} \ . \tag{3}$$

Then, one injects Eq. (2) into (1), multiplies by the complex conjugate of the z_h and ρ-dependent parts of Eq. (2), and finally integrates on these coordinates; one obtains the following differential equation for $f_e(z_e)$:[14,18]

$$\left[-\frac{\hbar^2}{2}\frac{\partial}{\partial z_e}\left[\frac{1}{m_{ez}}\frac{\partial}{\partial z_e}\right]V_e(z_e)+E_h+\frac{\hbar^2}{2\mu_\perp\alpha_\perp} -\frac{e^2}{\varepsilon_r}W(\alpha_\perp,z_e)\right]f_e(z_e)=E_X(\alpha_\perp)f_e(z_e) \ . \tag{4}$$

The effective attractive potential represented, e.g., in Fig. 1 of Ref. 14, is given by

$$W(\alpha_\perp,z_e)=\int_{-\infty}^{+\infty}dz_h|f_h(z_h)|^2\frac{2}{\alpha_\perp}S[2(z_e-z_h)/\alpha_\perp] \ , \tag{5a}$$

where

$$S(y)=\int_0^\infty dx\, x\frac{e^{-x}}{\sqrt{x^2+y^2}} \tag{5b}$$

can be easily fitted by a continued fraction. In practice, we replace the varying potential $W(\alpha_\perp,z_e)$ by a fitting stepwise function (we take steps of 0.1 nm in width). Then Eq. (4) can be solved by a classical transfer-matrix algorithm: inside each 0.1 nm wide "minilayer," $f_e(z_e)$ is a solution of a simple second-order differential equation, since both the potential and effective mass are constant. Thus $f_e(z_e)$ is a combination of plane or evanescent waves, whose wave vectors are connected to the energy by the dispersion relation, $k=(1/\hbar)[2m_e(E-W)]^{1/2}$. The eigenenergies are those that insure the conditions of continuity of $f_e(z_e)$ and of $(1/m_e)\partial f_e(z_e)/\partial z_e$ at all interfaces between "layers." The latter condition allows us to account for the mass mismatch between different materials[19,20] in a way that remains mathematically consistent with Eq. (4). The problem can be suppressed by taking identical masses in both materials, as apparently done in Ref. 14 (see, e.g., their Hamiltonian). Following this work, we will present results obtained within this approximation.

The fundamental confinement energy $E_X(\alpha_\perp)$ solution of Eq. (4) then has to be minimized over $\alpha_\perp$. The so-called binding energy of the exciton is simply given by $E_b=E_e+E_h-E_X$, where E_e is the confinement energy of a free electron in the potential well $V_e(z_e)$, in type-I structures. In type-II systems, since $V_e(z_e)$ is a potential barrier, one must let $E_e=0$. This procedure allows a parameter-free determination of the normalized envelope function $f_e(z_e)$ and, consequently of the excitonic oscillator strength, proportional to the probability P for finding the electron and the hole at the same point

$$P=\left|2/\alpha_\perp\int_{-\infty}^{+\infty}dz\, f_e(z)f_h(z)\right|^2 .$$

Involving a single variational parameter, this method provides a time-saving and quite accurate description of excitons in both type-I and type-II structures. Moreover, the use of a transfer-matrix algorithm allows a straightforward inclusion of perturbations such as electric fields.

Unfortunately, as discussed by Wu,[18] who first applied this formalism to type-I systems, using the 2D function of Eq. (3) gives less accurate results than using a 3D function, especially in the case of low band offsets. For usual type-I structures with deep and narrow enough quantum wells,[18,21] the strong confinement of both carriers governs the strengthening of Coulomb binding, so that the simpler 2D trial function is sufficient. We shall show in the following that this is not true for excitons in type-II quantum wells, essentially because of the large spatial extension of the wave function of the "outmost" carrier. For a "3D approximation," we thus replace Eq. (3) by

$$\varphi_{3\mathrm{D}}(\rho,z_e-z_h)=ce^{-[\rho^2+(z_e-z_h)^2]^{1/2}/\alpha} . \tag{6}$$

Now the 3D parameter α also partly controls the z extension of the electron, which is not the case for $\alpha_\perp$ in Eq. (3). The factor c must be extracted by normalization of the whole exciton function [Eq. (2)]. This needs the calculation of a triple integral over ρ, z_e, and z_h, contrary to the 2D case, because the in-plane and on-axis motions cannot be separated.

Following a similar procedure as that described above, $f_e(z_e)$ must satisfy the following differential equation:[18]

$$\left[-\frac{\hbar^2}{2}\frac{1}{m_{ez}}\frac{\partial^2}{\partial z_e^2}-A(\alpha,z_e)\frac{\partial}{\partial z_e}+V_e(z_e)+W(\alpha,z_e)+\frac{\hbar^2}{2\mu_\perp\alpha^2}+E_h\right]f_e(z_e)=E_X(\alpha)f_e(z_e) . \tag{7}$$

In addition to the effective potential $W(\alpha,z_e)$, we now have a first-derivative term, with factor $A(\alpha,z_e)$. This causes some difficulties concerning the problem of hermiticity due to mass discontinuities at interfaces. This is why we have chosen to write Eq. (7)—and especially its first term—in a way which is only strictly valid for z-independent masses. As stated above, we shall keep this approximation in the following numerical applications. The notations are the following:

$$W(\alpha,z_e)=2\left[\frac{\hbar^2}{2m_{ez}\alpha^2}(T_1-T_2)+\frac{\hbar^2}{\alpha^2}\left[\frac{1}{\mu_\perp}-\frac{1}{\mu_z}\right]Q-\frac{e^2}{\varepsilon_r\alpha}T_1\right]\Big/(T_1+T_2) , \tag{8a}$$

$$A(\alpha,z_e)=\frac{\hbar^2}{m_{ez}\alpha}\frac{T_3}{T_1+T_2} , \tag{8b}$$

where

$$T_j=\int_{-\infty}^{+\infty}dz_h|f_h(z_h)|^2\exp\left[-\frac{2}{\alpha}|z_e-z_h|\right]S_j \quad (j=1,2,3) , \tag{9a}$$

$$S_1=1 , \quad S_2=\frac{2}{\alpha}|z_e-z_h| , \quad S_3=\frac{2}{\alpha}(z_e-z_h) , \tag{9b}$$

$$Q=\int_{-\infty}^{+\infty}dz_h|f_h(z_h)|^2\frac{z^2}{\alpha^2}E_1\left[\frac{2|z_e-z_h|}{\alpha}\right] . \tag{9c}$$

$E_1(z)$ is the exponential integral.[22] Note that we have included the difference between in-plane and on-axis reduced masses, which was not done in Ref. 18. We have also corrected slight errors on mass denominators, in Eqs. (7) and (8a). Equation (7) is less easy to solve than Eq. (4), essentially because of the presence of the first-derivative term, which acts as a kind of viscous-friction term. Here again, we have simplified the numerical procedures by using a stepwise simulation of terms $W(\alpha,z_e)$ and $A(\alpha,z_e)$. Then, within each step layer, Eq. (7) has the form of a second-order differential equation with constant coefficients. The presence of the first-order term yields damp plane waves, i.e., the wave vector in each layer is complex, rather than purely real or imaginary. The boundary conditions are the same as those described above, so that a transfer-matrix algorithm can again be used for computing the eigenenergies and eigenfunctions. After the proper normalization of the whole exciton function $\Phi_{\mathrm{ex}}(\mathbf{r}_e,\mathbf{r}_h)$, the oscillator strength is obtained by a similar formulation as above, by simply replacing $2/\alpha_\perp$ by c.

III. RESULTS AND DISCUSSION

Figure 1 displays the comparison between 2D and 3D approximations. The binding energies of 1s excitons in GaAs-AlAs quantum wells are calculated versus the thickness of the GaAs layer. The strong anisotropy of longitudinal and transverse effective masses in X valleys is reasonable for the splitting into X_{xy} and X_z type-II excitons (see, e.g., Ref. 14), while a single type-I exciton exists for Γ_{6c}-Γ_{8v} electron-hole pairs. The numerical parameters, displayed in Table I, are those of Ref. 14, but image charge effects have not been included, for brevity, since they are of no interest for our purpose (anyway, their inclusion presents no difficulty). As stated above, the 3D model only yields a slight improvement for type-I Γ-like excitons, on account of the variational theorem, since E_b is increased by ~2%. On the other hand, a dramatic enhancement of E_b is obtained for type-II excitons. This

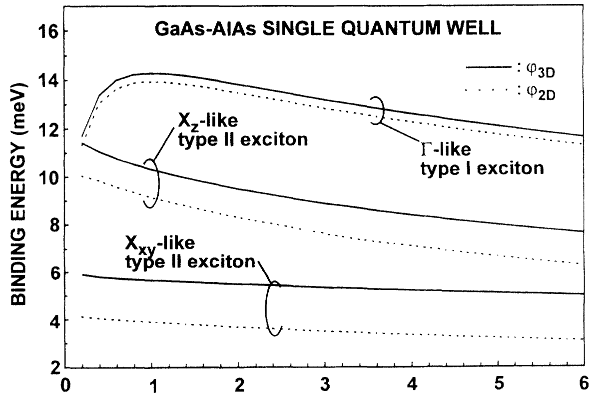

FIG. 1. Calculated binding energies of Γ-like type-I, X_z-like and X_{xy}-like type-II excitons in GaAs-AlAs quantum wells, versus the GaAs layer thickness. Dotted lines were obtained from Eq. (4), while solid curves result from Eq. (7). Image-charge effects were not included, for simplicity.

TABLE I. Numerical parameters used in our calculations of GaAs-AlAs quantum wells. For simplicity, effective masses for X electrons are those of AlAs, while we took GaAs values for heavy holes and Γ electrons. As stated in the text, these values are those taken by the authors of Ref. 14, for the sake of comparison.

Potential discontinuity for Γ electrons (meV)	1068
Potential discontinuity for X electrons (meV)	-197
Potential discontinuity for heavy holes (meV)	457
Γ-electrons effective mass (m_0)	0.067
X-electrons effective mass (m_0)	
longitudinal X_l	4.1
transverse X_t	0.19
heavy-hole effective mass (m_0)	0.37

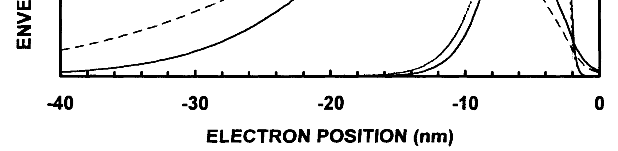

FIG. 2. The left-hand half of the "envelope function" $\tilde{f}_e(z_e)$ for a 4-nm-wide GaAs-AlAs quantum well. Both cases of X_z and X_{xy} excitons are shown. Solid lines represent the solutions obtained using the present 3D approximation, while dashed lines correspond to the 2D approach of Ref. 14. A thin dotted line shows the interface between GaAs and AlAs.

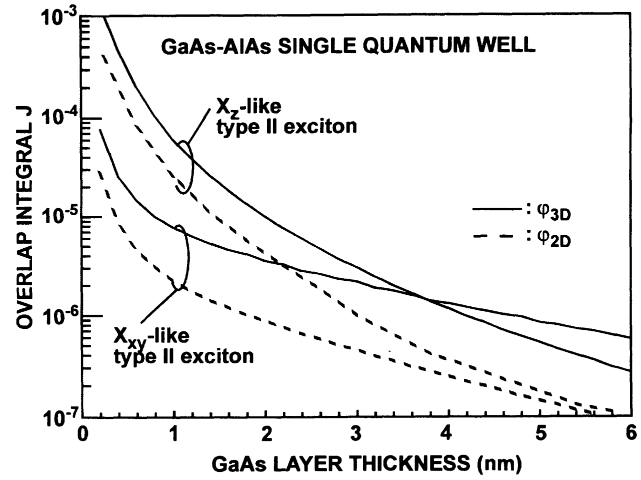

FIG. 3. Calculated values of the electron-hole overlap integral J, versus the thickness of the GaAs layer for the type-II excitons. The conditions are those of Fig. 1.

is explained by the fact that no confinement layer, but rather the Coulomb attraction itself, controls the spatial extension of the electron, especially along the z axis. This is why the z dependence of the relative motion must enter the hydrogenic part of the trial function. As evidence of this explanation, Fig. 1 shows that the enhancement of the binding energy is found smaller for X_z excitons ($\sim 18\%$), than for X_{xy} ones ($\sim 52\%$). This is due to the large value of the longitudinal effective mass for X_z valleys [$4.1 m_0$ (Ref. 14)], which insures that the X_z electron is maintained closer to the interface than the X_{xy} electron by the effective Coulomb attraction of the hole. This is confirmed by Fig. 2, which displays the left-hand half of the electron "envelope function" $\tilde{f}_e(z_e)$ calculated for the ground-state X-like excitons in a 4 nm wide GaAs-AlAs quantum well. Both 2D-like and 3D-like approximations are presented; $\tilde{f}_e(z_e)$ can be expressed as

$$\tilde{f}_e(z_e) = \left\{ \int \int \rho \, d\rho \, dz_h [f_h(z_h)]^2 \times [\varphi(\rho, z_e - z_h)]^2 [f_e(z_e)]^2 \right\}^{1/2} . \tag{10}$$

We have chosen to represent this function rather than the probability density, only because this allows a clearer view of the penetration of the electron in the GaAs layer. Note that the 2D-like approximation ($\varphi = \varphi_{2D}$) yields simply $\tilde{f}_e(z_e) = f_e(z_e)$. The difference between both approximations is dramatic: the spatial extension of the electron is quite smaller using the 3D model. This is particularly true for the X_{xy} electron, due to its smaller effective mass along z. Consequently, the improvement brought by the 3D approach is yet more eloquent when comparing squared electron-hole overlap integrals, displayed in Fig. 3, and obtained as

$$J = \left| \int_{-\infty}^{\infty} dz \, f_e(z) f_h(z) \varphi(0,0) \right|^2 . \tag{11}$$

These integrals are directly proportional to oscillator strengths for Γ-like and X_z-like direct excitons, and only give an indication of this strength for X_{xy}-like excitons,[14] which are indirect in k space. An order of magnitude can exist in favor of the 3D model. The reason for this is the very small overlap between the electron and hole wave functions, due to their short penetration across the interfaces. Any lack of precision on the exact behavior of these wave functions can have important consequences on the accuracy of the calculated overlap integrals. In particular, assuming, for simplicity, an infinite-well-like envelope function for the confined carrier, as done in Ref. 15, may yield correct binding energies but inaccurate oscillator strengths.

The 3D approach is thus far more accurate than the 2D one. This is particularly true for cases with very narrow or very shallow potential wells, or with small effective masses, where the large spatial extension of wave functions forbids the use of too drastic approximations.

IV. CONCLUSION

To summarize, we have used an adiabatic "effective-potential" approximation to calculate binding energies and oscillator strengths of type-II excitons. We have evidenced a dramatic improvement of accuracy, when choosing a 3D-like trial function instead of the usual 2D-like one. This improvement is proved by the important increment of binding energies, when comparing both hypotheses. We have shown that the choice of the 3D trial function is even more crucial for a correct estimation of oscillator strengths. The 3D model is strongly recommended, in particular, for an accurate treatment of type-I–to–type-II transitions which occur, for instance, in CdTe-(Cd,Mn)Te quantum wells, under magnetic fields.[15]

---

[1] G. Duggan and H. I. Ralph, Phys. Rev. B **35**, 4152 (1987).

[2] M. Matsuura and Y. Shinozuka, Phys. Rev. B **38**, 9830 (1988).

[3] B. R. Salmassi and G. E. W. Bauer, Phys. Rev. B **39**, 1970 (1989).

[4] M. M. Dignam and J. E. Sipe, Phys. Rev. B **41**, 2865 (1990).

[5] M. H. Degani and G. A. Farias, Phys. Rev. B **42**, 11 701 (1990).

[6] X. D. Zhang and K. K. Bajaj, Phys. Rev. B **44**, 10 913 (1991).

[7] S. V. Branis, J. Cen, and K. K. Bajaj, Phys. Rev. B **44**, 11 196 (1991).

[8] J. Cen, S.V. Branis, and K. K. Bajaj, Phys. Rev. B **44**, 12 848 (1991).

[9] S. V. Branis and K. I. Bajaj, Phys. Rev. B **45**, 6271 (1992).

[10] J. Cen and K. K. Bajaj, Phys. Rev. B **45**, 14 380 (1992).

[11] M. Cai, Y. Liu, W. Liu, and T. Yu, Physica B **176**, 327 (1992).

[12] T. Stirner, P. Harrison, W. E. Hagston, and J. P. Goodwin, J. Appl. Phys. **73**, 5081 (1993).

[13] G. Peter, E. Deleporte, G. Bastard, J.-M. Berroir, C. Delalande, B. Gil, J. M. Hong, and L. L. Chang, J. Lumin. **52**, 147 (1992).

[14] R. Zimmermann and D. Bimberg, Phys. Rev. B **47**, 15 789 (1993); J. Phys. IV **3**, 261 (1993).

[15] E. L. Ivchenko, A. V. Kavokin, V. P. Kochereshko, G. R. Posina, I. N. Uraltsez, D. R. Yakovlev, R. N. Bicknell-Tassius, A. Waag, and G. Landwehr, Phys. Rev. B **46**, 7713 (1992).

[16] See, for instance, P. Lefebvre, B. Gil, H. Mathieu, and R. Planel, Phys. Rev. B **39**, 5550 (1989); **40**, 7802 (1989), and references cited therein.

[17] See, for instance, J. Calatayud, J. Allègre, P. Lefebvre, and H. Mathieu, Mater. Sci. Eng. B **16**, 87 (1993), and references cited therein.

[18] J. W. Wu, Solid State Commun. **67**, 911 (1988).

[19] D. J. Ben Daniel and C. B. Duke, Phys. Rev. **152**, 683 (1966).

[20] G. Bastard, *Wave Mechanics Applied to Semiconductor Heterostructures* (Les Editions de Physique, Les Ulis, France, 1988), p. 112.

[21] G. Bastard, E. E. Mendez, L. L. Chang, and L. Esaki, Phys. Rev. B **26**, 1974 (1982).

[22] *Handbook of Mathematical Functions,* edited by M. Abramowitz and I. Stegun (Dover, New York, 1964), pp. 227–251.